European Radiology (2019) 29:6202–6210
https://doi.org/10.1007/s00330-019-06207-7

ONCOLOGY

Combination of intratumoural micellar paclitaxel with radiofrequency ablation: efficacy and toxicity in rodents

Hao Wu[1,2] · Zhi-Pu Fan[3] · An-Na Jiang[1] · Xing-Sheng Di[3] · Bing He[3] · Song Wang[1] · S. Nahum Goldberg[4,5] · Muneeb Ahmed[4] · Qiang Zhang[3] · Wei Yang[1]

Received: 10 August 2018 / Revised: 11 March 2019 / Accepted: 26 March 2019 / Published online: 16 April 2019

Abstract

Objectives To determine whether radiofrequency ablation (RFA) is more effective when combined with intratumoural injection (IT) than with intravenous injection (IV) of micelles.

Materials and methods Balb/c mice bearing 4T1 breast cancer were used. The tumour drug accumulation and biodistribution in major organs were evaluated at different time points after IT, IV, IT+RFA and IV+RFA. Periablational drug penetration was evaluated by quantitative analysis and pathologic staining after different treatments. For long-term outcomes, mice bearing tumours were randomised into six groups ($n = 7$/group): the control, IV, IT, RFA alone, IV+RFA and IT+RFA groups. The end-point survival was estimated for the different treatment groups.

Results In vivo, intratumoural drug accumulation was always much higher for IT than for IV within 48 h ($p < 0.001$). The IT+RFA group (3084.7 ± 985.5 μm) exhibited greater and deeper drug penetration than the IV+RFA group (686.3 ± 83.7 μm, $p < 0.001$). Quantitatively, the intratumoural drug accumulation in the IT+RFA group increased approximately 4.0-fold compared with that in the IV+RFA group ($p < 0.001$). In addition, compared with the IT treatment, the IT+RFA treatment further reduced the drug deposition in the main organs. Survival was longer in the IT+RFA group than in the IV+RFA ($p = 0.033$) and RF alone ($p = 0.003$) groups.

Conclusion The use of IT+RFA achieved much deeper and greater intratumoural drug penetration and accumulation, resulting in better efficacy, and decreased the systemic toxicity of nanoparticle-delivered chemotherapy.

Key Points

- *Association of IT+RFA achieved much deeper and greater intratumoural drug penetration than of IV+RFA, leading to better therapeutic efficacy.*
- *Compared with IV or IT chemotherapy alone, the combination with RFA decreased toxicity, especially in the IT+RFA group.*

Keywords Mice, inbred Babl/c · Micelles · Injections, intravenous · Injections, intralesional · Radiofrequency ablation

Hao Wu and Zhi-Pu Fan contributed equally to this work.

Electronic supplementary material The online version of this article (https://doi.org/10.1007/s00330-019-06207-7) contains supplementary material, which is available to authorized users.

✉ Wei Yang
13681408183@163.com

[1] Department of Ultrasound, Key Laboratory of Carcinogenesis and Translational Research (Ministry of Education /Beijing), Peking University Cancer Hospital & Institute, Beijing 100142, China

[2] Department of Ultrasonography, Guangdong Second Provincial General Hospital Affiliated to Southern Medical University, Guangzhou 510317, China

[3] State Key Laboratory of Natural and Biomimetic Drugs, School of Pharmaceutical Sciences, Peking University, Beijing 100191, China

[4] Laboratory for Minimally Invasive Tumor Therapies, Department of Radiology, Beth Israel Deaconess Medical Center, Harvard Medical School, Boston, MA 02215, USA

[5] Division of Image-Guided Therapy, Department of Radiology, Hadassah Hebrew University Medical Center, Jerusalem, Israel

Abbreviations

RFA Radiofrequency ablation
IT Intratumoural injection
IV Intravenous injection
PTX Paclitaxel

Introduction

Radiofrequency ablation (RFA) is a minimally invasive treatment for local tumours in the liver, lung, kidneys and other organs, with favourable outcomes in well-selected patients [1]. However, large tumours are challenging, due to the potential persistence of viable tumour cells in the margins or clefts of overlapping ablation zones, leading to local tumour progression, with an even reduced local efficacy in case of repeated ablation [2, 3]. Increasing the completeness of destruction would reduce residual lesions and increase survival [4–6].

One potential approach is the combination of RFA with nanoparticle-delivered chemotherapy. Previous preclinical studies indicated that combining RFA with liposomal chemotherapeutic agents induced larger tumour destruction, increased survival and enhanced tumour coagulation zones [4, 6, 7]. Many nanoparticles loaded with drugs, such as paclitaxel (PTX) [5], doxorubicin [8] and vinorelbine [9], have been used as an adjuvant to thermal ablation to enhance tumour cell death in the peripheral or transitional zone, where tumour cells possibly recover from reversible injury at sublethal temperatures.

However, the accumulation of nanocarriers in solid tumours via the enhanced permeability and retention (EPR) effect can be limited if the agent is delivered by intravenous injection (IV). For example, Plosker et al observed that the bioavailability of doxorubicin from Doxil (doxorubicin HCl liposome injection) reached only 40–50% and that the release rate was less than 5% in 24 h [10, 11]. Recently, one multicentre clinical study also showed that addition to RFA of an IV of thermosensitive liposomal doxorubicin did not increase the progression-free survival (PFS) and overall survival (OS) in patients with hepatocellular carcinoma (HCC) [12]. In addition, 24.2% of HCC patients in the clinical trial suffered from adverse events, such as alopecia, leukopenia and decreased neutrophil count. Therefore, solving the problem of low bioavailability and high drug toxicity with drug-loaded nanoparticles is needed.

To solve this problem, the potential solution of nanoparticle-delivered chemotherapy can be considered, namely changing the administration route [13–15]. Along these lines, we proposed direct intratumoural injection (IT) of nanoparticles, such as micelles. The rationale was to overcome limitations in tissue accumulation and penetration and to decrease the occurrence of adverse events. The purpose of this study was to compare the combination of RFA with drug-loaded micelles delivered through IT or IV in a rodent model and to determine if it can improve drug retention and interstitial penetration and lessen drug toxicity, with the aim to achieve a better treatment efficacy.

Materials and methods

The experimental animal protocol was first approved by the Institutional Animal Care and Use Committee. In this study, representative nanoparticles, specifically micelles (MI) loaded with paclitaxel (PTX), were prepared and characterised as an adjuvant agent combined with RFA, and Balb/c mice bearing 4T1 breast cancer were used. The detailed procedures are reported in our Supplementary materials. Our study was performed in different phases to systematically investigate the potential synergistic effects of RFA with IV- or IT-delivered MI.

In vivo fluorescence imaging and biodistribution

The PTX in micelles was replaced with DiR dyes to achieve better near-infrared (NIR) fluorescence imaging. When tumour volumes of mice reached approximately 500 mm^3, 4T1 tumour-bearing mice were randomly divided into two groups, which received 0.2 ml of micelles-DiR (10 mg/kg) via IV and via IT. At 1, 2, 4, 10, 24 and 48 h after injection, the mice ($n = 3$ for each time point) were anaesthetised with isoflurane and photographed using an imaging system (Carestream). After the final in vivo imaging, the mice were sacrificed immediately to harvest major organs (heart, liver, spleen, lung, kidneys). The ex vivo fluorescence images of all dissected organs were visualised with the same system and analysed with the Carestream MI software.

Intratumoural drug penetration for IV or IT when combined with RFA

To analyse the intratumoural penetration of micelles delivered through IT or IV with or without the addition of RFA (micelles loaded with DiD), mice were randomly divided into four groups ($n = 5$/group): (a) IT (0.2 ml micelles by IT), (b) IT+RFA (0.2 ml micelles by IT, followed by RFA after 24 h), (c) IV (0.2 ml micelles by IV) and (d) IV+RFA (0.2 ml micelles by IV, followed by RFA after 4 h). After treatment, the mice were sacrificed immediately to harvest tumour samples, and specimen slides of the tumour samples were prepared for drug tissue penetration by fluorescent dyes. The penetration thickness was considered the maximum distance within the tissue from the periablational zone where fluorescence occurs. The detailed procedures are reported in our Supplementary materials.

Quantitative analysis of periablational drug concentration

To further determine the periablational intratumoural drug concentration for the treatment with or without the addition of RFA, micelles entrapping PTX were administered according to the groups described above ($n = 3$/group). At 24 h after RFA, three mice in each group were sacrificed, and the tumours were harvested. Tumour tissue was ground, followed by PTX extraction and measurement by high-performance liquid chromatography (HPLC).

Drug biodistribution in organs for IV or IT when combined with RFA

In the study, we analysed the drug biodistribution in the organs for IT or IV combined with or without RFA (micelles loaded with DiR). Mice were randomly divided into four groups ($n = 5$/group) as follows: (a) IT (0.2 ml micelles by IT), (b) IT+RFA (0.2 ml micelles by IT, followed by RFA), (c) IV (0.2 ml micelles by IV) and (d) IV+RFA (0.2 ml micelles by IV, followed by RFA). After treatment, the mice were sacrificed immediately to harvest the main organs (heart, liver, spleen, lung, kidneys). The ex vivo fluorescence imaging of all dissected organs was performed and analysed with the Carestream MI software.

Long-term outcome and animal survival

Tumours measuring 10–12 mm were randomised into six experimental groups for tumour growth and end-point survival analysis ($n = 7$/group). These groups are (a) control (phosphate-buffered saline, PBS); (b) IT; (c) IV; (d) RFA alone; (e) IT+RFA and (f) IV+RFA. The mice receiving PBS without RFA or micelles were used as the control. The tumour volume and body weight of each mouse were recorded every 3 days for 3 weeks. The survival end-point was considered a tumour volume of 800 mm^3 or survival of 21 days, whichever was reached first. Secondary end-points were the rate of tumour growth and local control (i.e. no visible tumour on the abdominal wall). In addition, slices of tumour samples after treatment were stained with Ki-67 to evaluate the proliferation of tumour cells and with CD 31 (Cell Signalling Technology) to assess tumour vessels.

Statistical analysis

Continuous variables were presented as the mean ± SD and categorical variables as numbers and percentages. Student's t test and one-way ANOVA were used to compare the drug biodistribution in the tumour and main organs and the intratumoural drug penetration. Repeated measures analysis of variance was used to compare the tumour growth in different groups. The chi-square test and Fisher exact test were used to analyse Ki-67 and CD31 staining. Survival curves were constructed by the Kaplan-Meier method and compared by the log-rank test. Statistical significance was considered for a p value of less than 0.05. The statistical analysis was performed using SPSS 21.0 (SPSS Inc).

Results

In vivo fluorescence imaging and biodistribution

In vivo, tumour fluorescence was detected at 1 h after injection and remained at a high level in the IT group. The fluorescence signal intensity of the tumour increased in the IV group, reaching the maximum signal intensity at 24 h (Fig. 1a). The fluorescence signal intensity in the IT group was always much higher than that in the IV group within 48 h after injection ($p < 0.001$, Fig. 1b). The micelle biodistribution of micelle indicated that the greatest drug deposition occurred in the liver (Fig. 2a, b). Semi-quantitative analysis (Fig. 2c, d) showed that the fluorescence intensity in the liver was lower in the IT group than in the IV group at both 24 and 48 h after injection ($(103.0 \pm 4.4$ vs $170.3 \pm 30.0) \times 10^9$ phot/cm^2/s, $p < 0.001$ at 24 h; $(67.5 \pm 4.2$ vs $115.8 \pm 24.7) \times 10^9$ phot/cm^2/s, $p = 0.001$ at 48 h). For the heart, lung and kidney, the drug accumulation was also lower in the IT group than in the IV group at 24 h after injection ($(0.8 \pm 1.8$ vs $20.7 \pm 3.1) \times 10^9$ phot/cm^2/s $p = 0.005$ in the heart; $(49.5 \pm 8.0$ vs $69.3 \pm 16.1) \times 10^9$ phot/cm^2/s $p = 0.002$ in the lung and $(26.0 \pm 2.3$ vs $34.9 \pm 3.8) \times 10^9$ phot/cm^2/s, $p = 0.018$ in the kidney). At 48 h after injection, the fluorescence signal intensity of these organs decreased in both groups (Table 1).

Intratumoural drug penetration for IV or IT combined with RFA

Microscopic pathologic sections showed that the drug penetration was much more obvious in the IT+RFA group than the IT group, and the drug penetration was greater in the IV+RFA group than in the IV group (Fig. 3a). Semi-qualitative analysis also demonstrated that the IT+RFA treatment induced much greater and deeper tissue penetration (3084.7 ± 985.5 μm) than the IT treatment alone at 24 h after RFA (881.3 ± 240.1 μm, $p < 0.001$). In addition, the IV+RFA group (686.3 ± 83.7 μm) had deeper tissue penetration than the IV group alone (467.7 ± 215.9 μm, $p = 0.011$). Comparison of RFA combined the two types of injection showed deeper tissue penetration in the IT+RFA (3084.7 ± 985.5 μm) group than in the IV+RFA group (686.3 ± 83.7 μm, $p < 0.001$) (Fig. 3b, c).

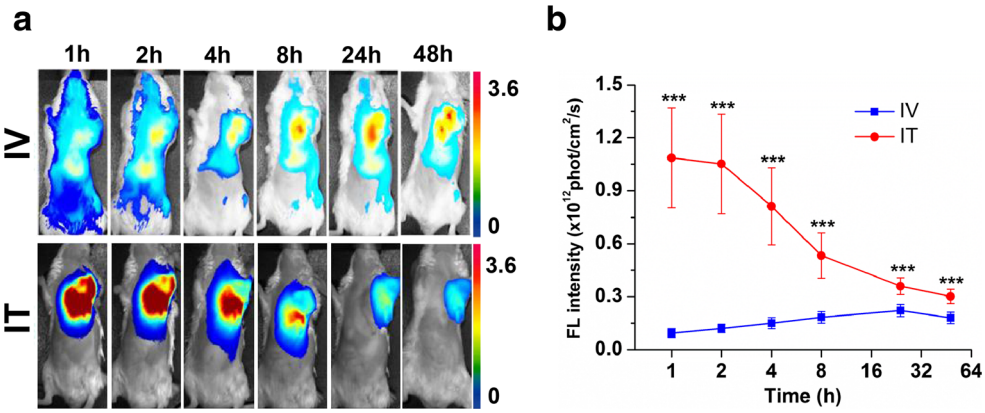

Fig. 1 In vivo fluorescence imaging and quantitative analysis. **a** The representative NIR fluorescence images in the different groups at the different time points. **b** Quantitative analysis of the fluorescence signal intensity in the different groups at the different time points (***$p < 0.001$, **$p < 0.01$). IV, intravenous; IT, intratumoural

Quantitative analysis of periablational drug concentration

To further qualitatively analyse the periablational drug concentration in tumours, PTX was measured in the tumour tissues treated with different methods (Fig. 4a). We observed a substantial increase in intratumoural PTX uptake at 24 h in tumours treated with RFA combined micelle-PTX for both IT and IV compared with that for micelle-PTX alone. The combination of RFA with micelle-PTX administration increased the intratumoural drug accumulation approximately 2.6-fold and 3.0-fold with IT and IV injection, respectively (8.19 ± 0.49 μg/g vs 3.14 ± 0.24 μg/g, $p < 0.001$; 2.06 ± 0.26 μg/g vs 0.69 ± 0.23 μg/g, $p < 0.001$).

Drug biodistribution in organs for IV or IT when combined with RFA

The semi-qualitative fluorescence intensity results for micelles in the main organs showed different kinetics and maximal levels of drug when combined with or without RFA (Fig. 4b). Compared with the IT group, the IT+RFA group achieved the lowest fluorescence intensity in every main organ at 48 h after injection ($p < 0.01$). This effect was most pronounced in the liver where the fluorescence intensity in the IT+RFA group decreased substantially compared with that in the IT group ($(42.5 \pm 1.7$ vs $102.9 \pm 43.6) \times 10^9$ phot/cm^2/s, $p < 0.001$). Similar fluorescence intensity decreases were found in comparison between the IV+RFA and IV groups. The maximal difference was observed between the IV+RFA and IV groups, where

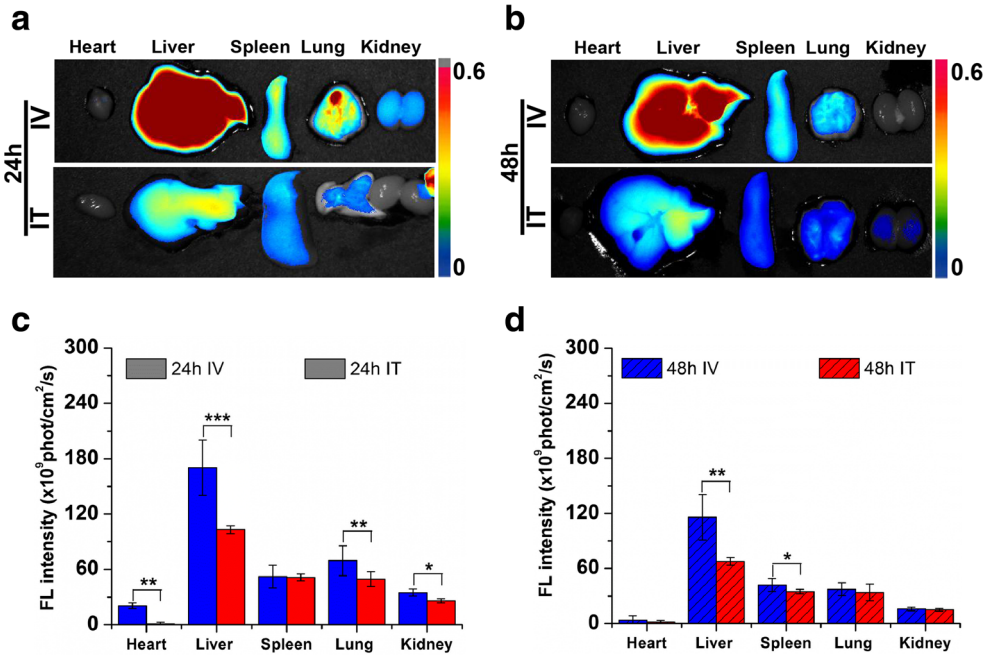

Fig. 2 The biodistribution of micelles in main organs after different administration routes. **a** The biodistribution of micelles in main organs at 24 h after IV and IT. **b** The biodistribution of micelles in main organs at 48 h after IV and IT. **c** The semi-quantitative analysis of the fluorescence intensity in main organs at 24 h after IV and IT. **d** The semi-quantitative analysis of the fluorescence intensity in main organs at 48 h after IV and IT (***$p < 0.001$, **$p < 0.01$, *$p < 0.05$)

Table 1 Fluorescence intensity of main organs at 24 h and 48 h after IV or IT injection ($\times 10^9$ phot/cm^2/s)

Organ	24 h IV	24 h IT	48 h IV	48 h IT
Heart	20.7 ± 3.1**	0.8 ± 1.8**	3.9 ± 4.6	1.8 ± 1.8
Liver	170.3 ± 30.0***	103.0 ± 4.4***	115.8 ± 24.7**	67.5 ± 4.2**
Spleen	52.2 ± 12.2	51.2 ± 3.5	42.2 ± 7.0*	34.9 ± 2.5*
Lung	69.3 ± 16.1**	49.5 ± 8.0**	37.5 ± 7.1	34.0 ± 9.1
Kidneys	34.9 ± 3.8*	26.0 ± 2.3*	16.0 ± 2.0	15.1 ± 1.5

Differences between IV injection and IT injection when compared at the same organs and time point were statistically significant (*$p < 0.05$, **$p < 0.01$, ***$p < 0.001$). *IT*, intratumoural; *IV*, intravenous

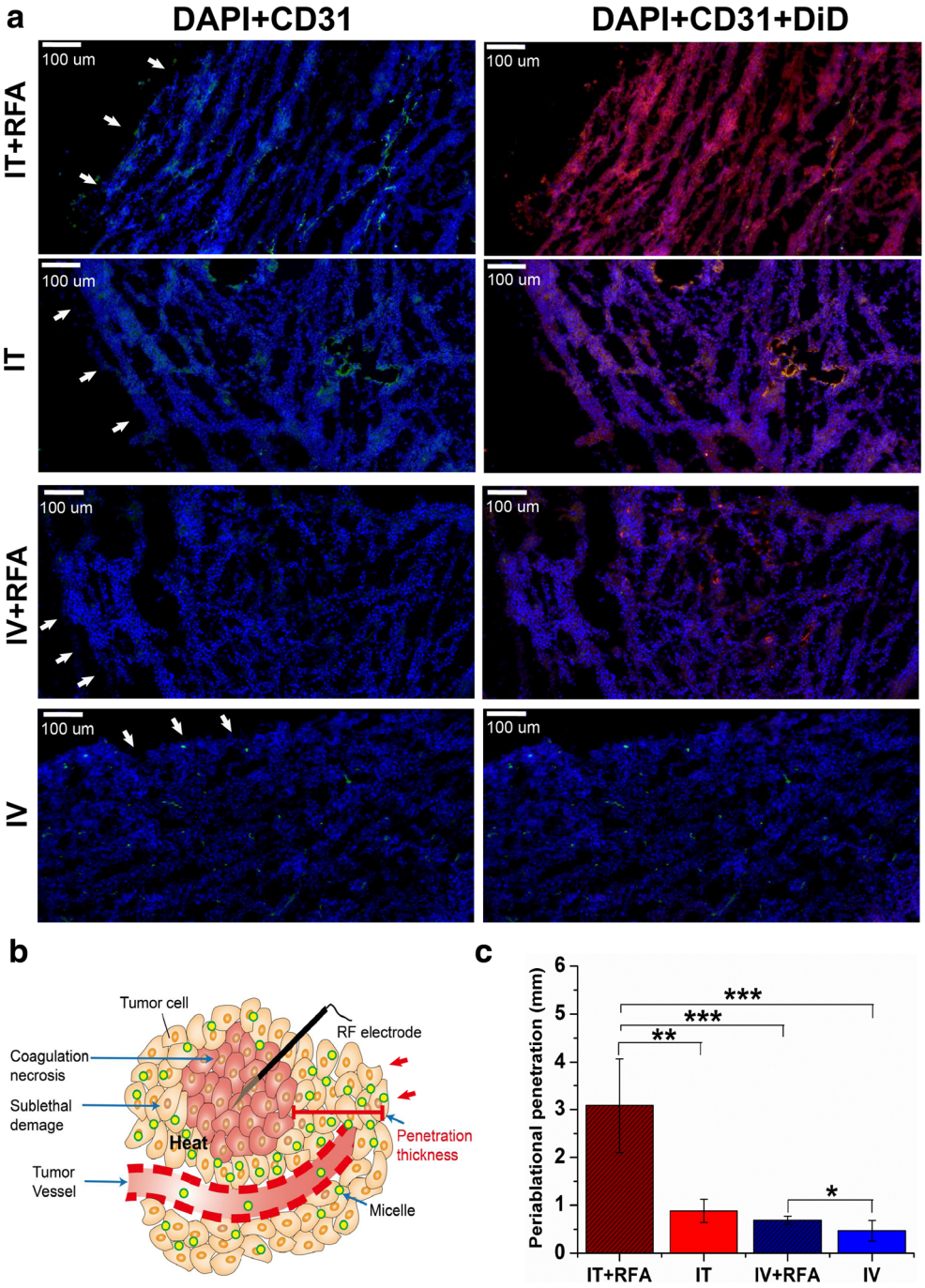

Fig. 3 Histologic analysis of drug penetration for IV and IT when combined with or without RFA. **a** The representative pictures of drug penetration in tumour tissue at different groups. Sections were stained with an anti-CD31 antibody (green) and DAPI (blue), and the native red fluorescence was used to detect DID. The white arrow marks the margin of tumour. Scale bars, 100 mm. **b** The diagrammatic sketch of measurement for the periablational penetration thickness, the red arrow marks the margin of tumour. **c** The penetration thickness was measured by software (**$p < 0.01$, ***$p < 0.001$)

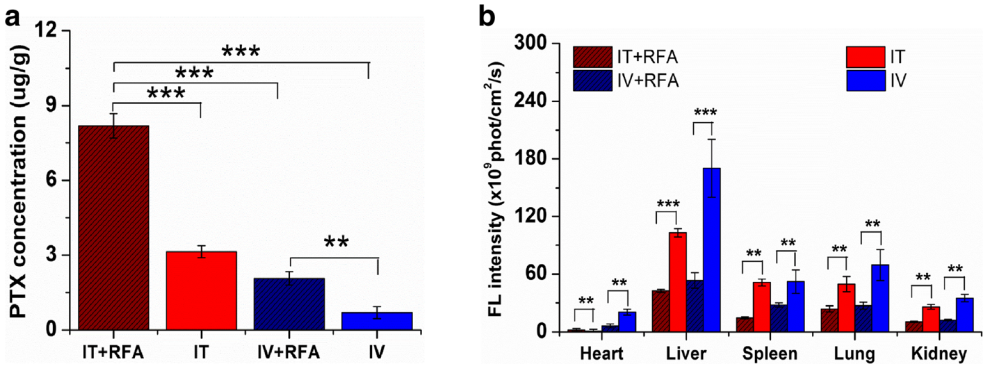

Fig. 4 Periablational intratumoural drug concentration and drug biodistribution in main organs for IV and IT when combined with or without RFA. **a** Qualitative analysis of the intratumoural PTX concentration in the different treatment groups. **b** The semi-quantitative analysis of the fluorescence intensity in main organs at 48 h after different treatments (***$p < 0.001$, **$p < 0.01$)

the fluorescence intensity of the liver in the IV group was 3.2-fold higher than that in the IV+RFA group ((53.3 ± 8.1 vs 170.3 ± 29.9) × 10^9 phot/cm^2/s, $p < 0.001$). Comparison of RFA combined the two types of injection showed lower liver fluorescence intensity was found in the IT+RFA group than in the IV+RFA group ((42.5 ± 1.7 vs 53.3 ± 8.1) × 10^9 phot/cm^2/s, $p = 0.001$).

Long-term outcome and histological analysis

As shown by the tumour growth curves (Fig. 5a), the tumour growth rate in the IT+RFA group was slowest compared with that in the IV+RFA group ($p = 0.005$) and the RFA alone group ($p < 0.001$). However, for the groups receiving micelles-PTX by IT or IV, the tumour inhibition efficiency

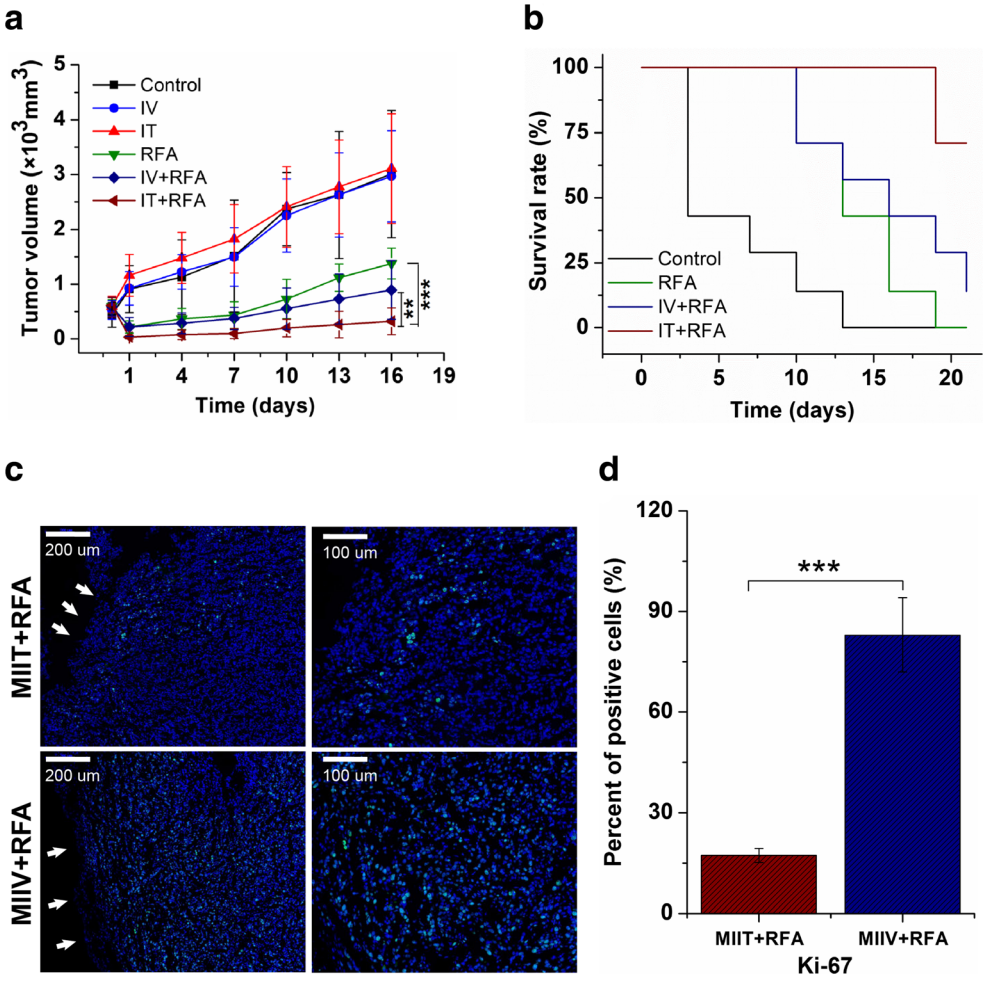

Fig. 5 Long-term outcomes and histological analysis after different treatments. **a** The tumour growth curves at different treatment groups. **b** The survival curves at different treatment groups. **c** The represented picture of Ki-67 staining after IT+RFA and IV+RFA. Sections were stained with an anti-CD31 antibody (green) and DAPI (blue) and the white arrow marks the margin of tumour. **d** The semi-qualitative analysis of Ki-67 staining in the IT+RFA group and IV+RFA group (***$p < 0.001$, **$p < 0.01$)

did not differ from that of the control (only PBS-treated) group ($p > 0.05$). Best local control also occurred in tumours treated with IT+RFA. The mice treated with IV+RFA and RFA showed only partial tumour growth inhibition during the first 9 days. Likewise, for end-point survival (Fig. 5b), the IT+RFA group had better survival than the IV+RFA group (20.4 ± 0.3 days vs 15.7 ± 1.8 days, $p = 0.033$) or the RFA alone group (20.4 ± 0.3 days vs 14.5 ± 1.3 days, $p = 0.003$). However, the IV+RFA and RFA groups had no substantial difference in their end-point survival ($p = 0.340$). In addition, Ki-67 staining in the periablational region showed less cell proliferation in the periablational viable area at 48 h in the IT+RFA group than in the IV+RFA group (17.3% ± 2.1% vs 83.0% ± 11.1%; $p < 0.001$) (Fig. 5c, d). CD31 staining in the periablational area also showed that the micro-vessel density in the IT+RFA group was sharply decreased compared with that in the IV+RFA group at 48 h (30.0 ± 9.6 vessels vs 125.0 ± 16.5 vessels, $p < 0.001$) (Fig. S4A-B).

Discussion

In the current study, small-sized micelles delivered via IT led to higher retention and persistent accumulation in tumours and a lower concentration in other healthy tissues compared with that of micelles delivered via IV. Tumour accumulation of drugs was always much higher in the IT group than in the IV group within 48 h after injection. Drug deposition in other organs was lower, especially the liver, in the IT group than in the IV group at 24 h and 48 h after injection. This was in agreement with the data from other groups using IT. For example, Phillips et al reported that compared with IV injection, IT administration induced greater intratumoural retention of ^{64}Cu nanoshells and less drug deposition in other healthy organs [16]. Likewise, Bao et al also showed that higher intratumoural retention of ^{99m}Tc liposomes was achieved by intratumourally administered liposomal drugs [14]. Our study demonstrated that the combination with RFA was beneficial for increasing drug penetration: the IT+RFA group exhibited greater and deeper tissue penetration than those of the IT group alone. Quantitative measurement indicated that the periablational drug concentration in the IT+RFA group was approximately 2.6-fold higher than that in the IT group. Overall, this effect was probably the consequence of heat-induced injury in the periablation zone [17].

Several studies showed that an increased interstitial fluid pressure (IFP) resulting from vessel abnormalities, fibrosis and contraction of the interstitial matrix in tumours formed a barrier to delivery transport, thus resulting in inefficient uptake and penetration of therapeutic agents [18, 19]. Some studies demonstrated the IFP can decrease markedly, causing an increase in the net filtration pressure in certain pathological conditions, such as inflammation or burn injuries [20, 21]. RFA produces acute inflammation from heat injury, possibly inducing a decrease in the IFP which might explain in part the increased penetration of drug-loaded micelles in our study. Sublethal damage from RFA also affects the contractile function of tumour stromal fibroblasts, contributing to a lower IFP by preventing them to bind to the collagen fibres in an integrin-dependent manner which would increase tension between the fibres [18, 22].

Greater drug accumulation and longer retention time were also essential to achieving the favourable intratumoural drug penetration when combined with RFA. During follow-up, tumour growth was obviously inhibited in the IT+RFA group, while in the IV+RFA group, the tumours relapsed at 9 days after RFA. These results were also confirmed by the histological analysis that the expression of Ki-67 and CD31 in the periablational region was lower in the IT+RFA group than that in the IV+RFA group at 48 h after treatment. One interpretation of this phenomenon is that the better drug accumulation and retention from IT administration provided the basis for the deeper drug penetration when combined with RFA. According to the tumour growth curves, tumour growth did not differ significantly among the three groups without RFA while IT+RFA had significantly slower growth than IV+RFA, which further proved that the combination of RFA with intratumoural administration was the key for achieving better drug penetration and treatment efficacy.

While these results are exciting in achieving the primary goal of combining RFA with micelles delivered via IT, the micelle biodistribution in main organs was also needed for evaluating the systemic toxicity. As mentioned above, the concentration of drug deposited in the main organs was certainly much lower in the IT group than in the IV group. We found that the addition of RFA further decreased the drug deposition in the main organs, especially in the IT+RFA group. The phenomenon may be interpreted as follows: as RFA facilitates its accumulation within the tumour, drug leakage into the circulation and consequently deposition in other organs decreases [17, 23–25]. Similar studies reported that longer hyperthermia time span may be essential to enhance drug accumulation in the tumour and decrease drug plasmatic level and deposition in main organs [26, 27].

There were several limitations in this study. First, this study did not include a free paclitaxel-alone arm. However, previous studies had clearly demonstrated that intratumoural administration of free chemotherapeutic drug (e.g. paclitaxel) failed to achieve longer retention in the tumour because of the low molecular weight of the free drug, ultimately resulting in rapid clearance and no significant improvement in antitumour efficacy [13, 28]. Additionally, although 4T1 tumour model used in our studies is a well-characterised tumour model, the results may be specific to the model and thus should be interpreted and applied to other scenarios and models with caution. Different tumours may potentially have different levels of

"porosity" and drug retention characteristics [29–31]. Moreover, the injection dose and time point in combination therapy will play an important role in future work.

In conclusion, the use of IT+RFA led to much deeper and greater intratumoural drug penetration and accumulation, resulting in better therapeutic efficacy. Compared with IV or IT chemotherapy alone, the combination with RFA decreased toxicity, especially in the IT+RFA group.

Funding This study has received funding by the National Natural Science Foundation of China (Grant Nos. 81471768, 81773286, 81571674 and 81771853).

Compliance with ethical standards

Guarantor The scientific guarantor of this publication is Yang Wei.

Conflict of interest One author (S.N.G.) receives consulting fees from Angiodynamics and Cosman Company. These companies had no control or involvement in data collection, data analysis, or manuscript preparation. Other authors had no conflict of interest and had unrestricted control of study data.

Statistics and biometry Goldberg SN, Ahmed Muneeb and Zhang Qiang kindly provided statistical and constructive advice for this manuscript.

Informed consent Approval from the institutional animal care committee was obtained.

Ethical approval Institutional Review Board approval was obtained.

Methodology
- Experimental
- Performed at one institution

References

1. Ahmed M, Brace CL, Lee FT Jr, Goldberg SN (2011) Principles of and advances in percutaneous ablation. Radiology 258:351–369
2. Sofocleous CT, Nascimento RG, Petrovic LM et al (2008) Histopathologic and immunohistochemical features of tissue adherent to multitined electrodes after RF ablation of liver malignancies can help predict local tumor progression: initial results. Radiology 249:364–374
3. Ni JY, Liu SS, Xu LF, Sun HL, Chen YT (2013) Meta-analysis of radiofrequency ablation in combination with transarterial chemoembolization for hepatocellular carcinoma. World J Gastroenterol 19:3872–3882
4. Ahmed M, Goldberg SN (2004) Combination radiofrequency thermal ablation and adjuvant IV liposomal doxorubicin increases tissue coagulation and intratumoural drug accumulation. Int J Hyperthermia 20:781–802
5. Yang W, Ahmed M, Elian M et al (2010) Do liposomal apoptotic enhancers increase tumor coagulation and end-point survival in percutaneous radiofrequency ablation of tumors in a rat tumor model? Radiology 257:685–696
6. Ahmed M, Liu Z, Lukyanov AN et al (2005) Combination radiofrequency ablation with intratumoral liposomal doxorubicin: effect on drug accumulation and coagulation in multiple tissues and tumor types in animals. Radiology 235:469–477
7. D'Ippolito G, Ahmed M, Girnun GD et al (2003) Percutaneous tumor ablation: reduced tumor growth with combined radiofrequency ablation and liposomal doxorubicin in a rat breast tumor model. Radiology 228:112–118
8. Ahmed M, Monsky WE, Girnun G et al (2003) Radiofrequency thermal ablation sharply increases intratumoral liposomal doxorubicin accumulation and tumor coagulation. Cancer Res 63:6327–6333
9. Wang S, Mei XG, Goldberg SN et al (2016) Does thermosensitive liposomal vinorelbine improve end-point survival after percutaneous radiofrequency ablation of liver tumors in a mouse model? Radiology 279:762–772
10. Plosker GL (2008) Pegylated liposomal doxorubicin: a review of its use in the treatment of relapsed or refractory multiple myeloma. Drugs 68:2535–2551
11. Gabizon A, Shmeeda H, Barenholz Y (2003) Pharmacokinetics of pegylated liposomal doxorubicin: review of animal and human studies. Clin Pharmacokinet 42:419–436
12. Tak WY, Lin SM, Wang Y et al (2018) Phase III HEAT study adding lyso-thermosensitive liposomal doxorubicin to radiofrequency ablation in patients with unresectable hepatocellular carcinoma lesions. Clin Cancer Res 24:73–83
13. Li X, Li R, Qian X et al (2008) Superior antitumor efficiency of cisplatin-loaded nanoparticles by intratumoral delivery with decreased tumor metabolism rate. Eur J Pharm Biopharm 70:726–734
14. Bao A, Phillips WT, Goins B et al (2006) Potential use of drug carried-liposomes for cancer therapy via direct intratumoral injection. Int J Pharm 316:162–169
15. Wong C, Stylianopoulos T, Cui J et al (2011) Multistage nanoparticle delivery system for deep penetration into tumor tissue. Proc Natl Acad Sci U S A 108:2426–2431
16. Xie H, Goins B, Bao A, Wang ZJ, Phillips WT (2012) Effect of intratumoral administration on biodistribution of 64Cu-labeled nanoshells. Int J Nanomedicine 7:2227–2238
17. Nikfarjam M, Muralidharan V, Christophi C (2005) Mechanisms of focal heat destruction of liver tumors. J Surg Res 127:208–223
18. Heldin CH, Rubin K, Pietras K, Ostman A (2004) High interstitial fluid pressure - an obstacle in cancer therapy. Nat Rev Cancer 4:806–813
19. Prabhakar U, Maeda H, Jain RK et al (2013) Challenges and key considerations of the enhanced permeability and retention effect for nanomedicine drug delivery in oncology. Cancer Res 73:2412–2417
20. Lund T, Wiig H, Reed RK (1988) Acute postburn edema: role of strongly negative interstitial fluid pressure. Am J Physiol 255:H1069–H1074
21. Kristensen CA, Nozue M, Boucher Y et al (1996) Reduction of interstitial fluid pressure after TNF-alpha treatment of three human melanoma xenografts. Br J Cancer 74:533–536
22. Gabbiani G (2003) The myofibroblast in wound healing and fibrocontractive diseases. J Pathol 200:500–503
23. Knavel EM, Brace CL (2013) Tumor ablation: common modalities and general practices. Tech Vasc Interv Radiol 16:192–200
24. Kruskal JB, Oliver B, Huertas JC, Goldberg SN (2001) Dynamic intrahepatic flow and cellular alterations during radiofrequency ablation of liver tissue in mice. J Vasc Interv Radiol 12:1193–1201
25. Kong G, Anyarambhatla G, Petros WP et al (2000) Efficacy of liposomes and hyperthermia in a human tumor xenograft model: importance of triggered drug release. Cancer Res 60:6950–6957
26. Grüll H, Langereis S (2012) Hyperthermia-triggered drug delivery from temperature-sensitive liposomes using MRI-guided high intensity focused ultrasound. J Control Release 161:317–327

27. Li L, ten Hagen TL, Bolkestein M et al (2013) Improved intratumoral nanoparticle extravasation and penetration by mild hyperthermia. J Control Release 167:130–137
28. Ning S, Yu N, Brown DM, Kanekal S, Knox SJ (1999) Radiosensitization by intratumoral administration of cisplatin in a sustained-release drug delivery system. Radiother Oncol 50:215–223
29. Maruyama K (2011) Intracellular targeting delivery of liposomal drugs to solid tumors based on EPR effects. Adv Drug Deliv Rev 18:161–169
30. Santagiuliana R, Pereira RC, Schrefler BA, Decuzzi P (2018) Predicting the role of microstructural and biomechanical cues in tumor growth and spreading. Int J Numer Method Biomed Eng 34:e2935
31. Rajabi M, Mousa SA (2017) The role of angiogenesis in cancer treatment. Biomedicines 5:34